Mdm2 phosphorylation by Akt regulates the p53 response to oxidative stress to promote cell proliferation and tumorigenesis

Loretah Chibaya[a,b], Baktiar Karim[c], Hong Zhang[a,b], and Stephen N. Jones[a,b,c,1]

[a]Department of Cell and Developmental Biology, University of Massachusetts Medical School, Worcester, MA 01655; [b]Department of Pediatrics, University of Massachusetts Medical School, Worcester, MA 01655; and [c]Laboratory Animal Sciences Program, Frederick National Laboratory for Cancer Research, Frederick, MD 21702

Edited by Carol Prives, Columbia University, New York, NY, and approved November 23, 2020 (received for review February 19, 2020)

We have shown previously that phosphorylation of Mdm2 by ATM and c-Abl regulates Mdm2-p53 signaling and alters the effects of DNA damage in mice, including bone marrow failure and tumorigenesis induced by ionizing radiation. Here, we examine the physiological effects of Mdm2 phosphorylation by Akt, another DNA damage effector kinase. Surprisingly, Akt phosphorylation of Mdm2 does not alter the p53-mediated effects of ionizing radiation in cells or mice but regulates the p53 response to oxidative stress. Akt phosphorylation of Mdm2 serine residue 183 increases nuclear Mdm2 stability, decreases p53 levels, and prevents senescence in primary cells exposed to reactive oxidative species (ROS). Using multiple mouse models of ROS-induced cancer, we show that Mdm2 phosphorylation by Akt reduces senescence to promote $Kras^{G12D}$-driven lung cancers and carcinogen-induced papilloma and hepatocellular carcinomas. Collectively, we document a unique physiologic role for Akt-Mdm2-p53 signaling in regulating cell growth and tumorigenesis in response to oxidative stress.

Mdm2 | Akt | senescence | Tp53 | tumorigenesis

The p53 tumor suppressor is commonly mutated or functionally inactivated in a wide variety of human cancers. Humans and mice who inherit a mutant p53 allele exhibit an enhanced susceptibility to tumorigenesis (1) and frequently display somatic mutations of the wild-type (WT) p53 allele. The ability of p53 to suppress tumorigenesis is largely linked to the ability of p53 to regulate the transcription of numerous genes involved in apoptosis, cell cycle arrest, senescence, and DNA repair (2). These various and potent p53 functions are kept in check under homeostatic conditions by the Mdm2 oncoprotein, which complexes with p53 and sterically inhibits p53 transcriptional activity (3). Mdm2 also inhibits p53 activities by promoting p53 nuclear export (4) and by acting as an E3 ubiquitin ligase to target p53 for 26S proteasomal degradation (5). However, in cells exposed to various forms of genotoxic or metabolic stress, the p53 protein is posttranslationally modified and stabilized, and p53 transcriptional activities are greatly elevated. Since Mdm2 gene expression is also transactivated by p53, subsequent Mdm2-p53 signaling helps p53 functions return to normal homeostatic levels after cessation of the cell stress response (6). The importance of the Mdm2-p53 signaling axis in regulating p53 activities has been highlighted in vivo by the rescue of Mdm2-deficient mice from early embryonic lethality by codeletion of p53 and by the unchecked cell stress responses induced by p53 in numerous mouse tissues conditionally ablated for Mdm2 (7).

Mdm2-p53 signaling is regulated during the DNA damage response (DDR) by posttranslational modification of p53. For example, effector kinases such as ATM can phosphorylate p53 after DNA damage (7). However, mouse modeling experiments have revealed that these modifications have only a modest effect on Mdm2 or p53 protein levels and mainly promote the ability of p53 to transactivate heterologous gene expression (8, 9). In contrast, we have shown that ATM phosphorylation of Mdm2 on serine residue 394 can greatly alter Mdm2 and p53 protein levels and p53 activities in cells and in mice treated with ionizing radiation (IR) (10). The c-Abl kinase is also capable of phosphorylating Mdm2 after DNA damage on tyrosine residue 393, and phosphorylation of Mdm2 by either ATM (Ser394) or cAbl (Tyr393) impacts p53 functions in hematopoietic stem cells to alter bone marrow failure and tumorigenesis in mice after whole-body IR exposure (10–12). These studies demonstrate that phosphorylation of Mdm2 is central to the ability of these DNA damage effector kinases to transduce growth arrest and cell death signals following DNA damage induced by IR.

AKT, a serine/threonine kinase within the receptor tyrosine kinase/phosphatase and tensin homolog (PTEN)/phospho-inositide 3-kinase (PI3K) pathway, also contributes to DDR signaling. AKT (Akt in mice) is activated by growth factor signaling and by cell stress and regulates a number of cellular functions, including cell growth control, apoptosis, and DNA repair (13). In addition, Akt can be activated by DNA damaging agents, including IR and chemotherapeutic agents such as doxorubicin (14), resulting in impaired DNA repair and the radiosensitization of cancers (15). A role for AKT-Mdm2 signaling in the DNA damage response has also been proposed due to the ability of AKT to phosphorylate human MDM2 (16, 17). In vitro studies have revealed that AKT phosphorylation of MDM2 at either Ser166 and/or Ser186 promotes MDM2 translocation into the nucleus (16, 18) and reduces p53-dependent gene transactivation (16). AKT-mediated phosphorylation of MDM2 has also been reported to enhance MDM2's ability to ubiquitinate and degrade p53 (17). These cell-based studies suggest that AKT-MDM2 signaling may participate in the DNA damage response of cells to IR.

Significance

We demonstrate that Akt phosphorylation of Mdm2 protein at Ser183 inhibits p53-mediated senescence and promotes ROS-induced tumorigenesis. Thus, different effector kinases can modify Mdm2 and selectively regulate the p53-mediated response to stress. Our study suggests that targeted inhibition of Mdm2 Ser183 phosphorylation would activate p53-mediated senescence and delay tumor progression.

Author contributions: L.C., H.Z., and S.N.J. designed research; L.C. performed research; L.C. and B.K. analyzed data; L.C., H.Z., and S.N.J. wrote the paper; and B.K. performed tumor histopathology.

The authors declare no competing interest.

This article is a PNAS Direct Submission.

[1]To whom correspondence may be addressed. Email: stephen.jones2@nih.gov.

This article contains supporting information online at https://www.pnas.org/lookup/suppl/doi:10.1073/pnas.2003193118/-/DCSupplemental.

Published January 19, 2021.

To explore further a role of Akt phosphorylation of Mdm2 in the regulation of p53 in the DDR and in p53-mediated tumor suppression, we generated two mouse models expressing Mdm2 that cannot be selectively phosphorylated at either Ser163 or Ser183 (the murine equivalents of human MDM2 Ser166 and Ser186). Surprisingly, we found that Akt phosphorylation of Mdm2 did not alter the response of cells or mice to IR. However, our studies reveal that Akt phosphorylation of Mdm2 Ser183 (but not Mdm2 Ser163) prevents premature senescence in primary cells triggered by exposure to oxidative stress. In contrast to the inhibitory effects of other DDR effector kinases on endogenous Mdm2 stability, phosphorylation of Mdm2 Ser183 by Akt promotes Mdm2 stability, resulting in increased nuclear levels of Mdm2, reduced nuclear levels of p53, and enhanced cell growth. In keeping with a role for Mdm2 phosphorylation by Akt in regulating the growth of cells exposed to oxidative stress, tumorigenesis in multiple mouse models of oxidative stress-induced cancer is greatly reduced in $Mdm2^{S183A}$ mice.

Results

Phosphorylation of Mdm2 Ser163 or Mdm2 Ser183 Is Not Required for Mouse Embryonic Development. To investigate how Akt phosphorylation of Mdm2-Ser163 or Mdm2-Ser183 regulates Mdm2-p53 signaling in vivo, we utilized CRISPR-mediated genome editing to generate mice with alanine residues at either position. C57BL/6 zygotes were injected with Cas9 mRNA, gRNAs with complementary sequences to regions corresponding to either Ser163 or Ser183 residue, and 100mer oligonucleotides with sequences encoding either Ala163 or Ala183 (*SI Appendix*, Fig. S1*A*). Since successful genome editing also generates new restriction enzyme sites (*SI Appendix*, Fig. S1*B*), the mutant Mdm2 alleles can be distinguished by restriction enzyme digestion of PCR products containing the regions with the targeted mutations (*SI Appendix*, Fig. S1*C*). Injected blastocysts were transplanted into pseudopregnant mice, and mice bearing the Mdm2 S163A or Mdm2 S183A allele were recovered. Heterozygous ($Mdm2^{S163A/+}$ and $Mdm2^{S183A/+}$) mice were backcrossed with C57BL/6 WT mice for six and nine generations, respectively, to eliminate potential CRISPR off-target mutations. The intended Mdm2 mutations were confirmed by sequencing of genomic regions corresponding to Mdm2 Ser163 or Mdm2 Ser183 (*SI Appendix*, Fig. S1*D*). In addition, sequencing of Mdm2 cDNA confirmed that no mutations were present in Mdm2's coding regions other than the intended Mdm2 S163A or Mdm2 S183A mutations. Progenies from either heterozygous $Mdm2^{S163A/+}$ or heterozygous $Mdm2^{S183A/+}$ intercrosses were recovered at Mendelian ratios (*SI Appendix*, Fig. S1*E*), and male and female progenies were generated at similar (50%) frequencies. Unlike Mdm2-null mice which are embryonic lethal (19, 20), homozygous $Mdm2^{S163A/S163A}$ and $Mdm2^{S183A/S183A}$ (hereafter referred as $Mdm2^{S163A}$ and $Mdm2^{S183A}$) mice were viable, fertile, and showed similar body weight to WT mice (*SI Appendix*, Fig. S1*F*). Taken together, these data suggest that Akt phosphorylation of Mdm2 at either Ser163 or Ser183 is dispensable for the development and normal growth of mice.

Phosphorylation of Mdm2 Ser183 Is Required for Cell Proliferation under Oxidative Stress. Previous studies suggest that phosphorylation of human MDM2 by Akt at either Ser166 or Ser186 alters its subcellular localization and results in increased p53 protein levels (16, 18). To determine whether phosphorylation of Mdm2 Ser163 or Mdm2 Ser183 modified p53 levels and cell proliferation, we generated mouse embryonic fibroblasts (MEFs) from WT, $Mdm2^{S163A}$, $Mdm2^{S183A}$, and $p53^{-/-}$ embryos at embryonic day 13.5 (E13.5). Interestingly, $Mdm2^{S183A}$ MEFs failed to proliferate (Fig. 1*A*) and were unable to form colonies when plated at low density (Fig. 1*B*). This failure was not due to increased apoptosis, as there were no significant differences in the percentage of apoptotic cells among WT, $Mdm2^{S163A}$, and $Mdm2^{S183A}$ MEFs as determined by Annexin V and propidium iodide (PI) staining (*SI Appendix*, Fig. S3*A*). Instead, $Mdm2^{S183A}$ MEFs exhibited a senescent morphology. Senescence associated β-galactosidase (SA-β-gal) staining revealed that $Mdm2^{S183A}$ MEFs had a 12-fold increase in the number of cells staining positive for SA-β-gal, relative to WT MEFs or $Mdm2^{S163A}$ MEFs, and a 30-fold increase compared to $p53^{-/-}$ MEFs (Fig. 1*C*). These results indicate that loss of phosphorylation of Mdm2 Ser183 triggers premature senescence in MEFs grown under conventional tissue culture conditions. In contrast, cells and mice bearing the $Mdm2^{S163A}$ allele displayed no unusual phenotypes. In keeping with literature highlighting a role for Akt in promoting cell growth (13), we found that inhibiting Akt with MK-2206 reduced the proliferation of WT MEFs (*SI Appendix*, Fig. S2*A*). However, reduced proliferation in WT MEFs was not due to senescence (*SI Appendix*, Fig. S2 *B* and *C*), suggesting that other compensatory pathways that can no longer be engaged in $Mdm2^{S183A}$ MEFs may be activated in WT MEFs. It is possible these pathways may activate other kinases capable of phosphorylating Mdm2 Ser183 in WT MEFs. These findings are consistent with previous studies that demonstrated that loss of Akt expression does not lead to senescence in early passage WT MEFs (21).

Cellular senescence can be triggered by many stimuli, including telomere erosion, aberrant oncogenic signaling, DNA damage, oxidative stress, and inflammation (22). Given that the difference in the growth of the primary cells was not reflected by differences in the growth of mice, we posited that $Mdm2^{S183A}$ MEFs were senescent due to their enhanced sensitivity to oxidative stress. To test this hypothesis, we cultured WT, $Mdm2^{S183A}$ MEFs at low oxygen (5%) in media supplemented with various concentrations of *N*-acetyl-cysteine (NAC), a scavenger of reactive oxygen species (ROS). While 2.5 mM NAC supplemented in media partially rescued the growth of mutant cells, we found that 5 mM NAC largely rescued the proliferative defect of $Mdm2^{S183A}$ MEFs with no negative effect on cell viability, unlike what was seen with 10 mM NAC (*SI Appendix*, Fig. S3*C*). In MEFs cultured at 5% oxygen with 5 mM NAC, there was no difference in the proliferation of WT and $Mdm2^{S183A}$ MEFs (Fig. 1*D*), and $Mdm2^{S183A}$ MEFs were able to form colonies at low density, albeit at lower frequency than WT (Fig. 1*E*). There were no differences in apoptosis in $Mdm2^{S183A}$ and WT MEFs under low oxygen condition (*SI Appendix*, Fig. S3*B*), and low oxygen conditions greatly reduced the percentage of SA-β-gal-positive cells in $Mdm2^{S183A}$ MEFs (8.9%) (Fig. 1*F*) compared to 58.9% (Fig. 1*C*) when cultured under conventional culture conditions (~21% O_2). Further, supplementing the media with 5 mM NAC at high oxygen (~21%) failed to rescue defective cell proliferation (*SI Appendix*, Fig. S3*D*) and premature senescence (*SI Appendix*, Fig. S3*E*) in $Mdm2^{S183A}$ MEFs. These data indicate that lowering the oxygen tension to 5% and reducing ROS levels with 5 mM NAC rescued the proliferative defect and premature senescence of $Mdm2^{S183A}$ MEFs seen in conventional high oxygen (~21% O_2) culture conditions.

We examined the expression of senescence-associated markers in low passage (3) $Mdm2^{S183A}$ MEFs, including p16, p21, and p53. The level of p53, phosphorylated p53 (S18), p21, and p16 proteins were significantly elevated in $Mdm2^{S183A}$ MEFs compared to WT MEFs when plated at high oxygen (Fig. 2*A*). Similarly, mRNA levels of p53 targets p21, Pai-1, Pai-2, but not Mdm2, Sestrin-1, and Sestrin-2, were significantly elevated in $Mdm2^{S183A}$ MEFs compared to WT MEFs at high oxygen (Fig. 2*B*). Up-regulation of these senescence markers in $Mdm2^{S183A}$ MEFs was greatly reduced when the cells were grown in low oxygen conditions (Fig. 2*C*), and the mRNA levels of p53-target genes such as p21, Pai-1, and Pai-2 in $Mdm2^{S183A}$ MEFs were not different from levels observed in WT MEFs (Fig. 2*D*). These data indicate that differences in the amount of WT and mutant Mdm2 gene expression does not account for the differences in Mdm2 or p53 protein levels, and that premature

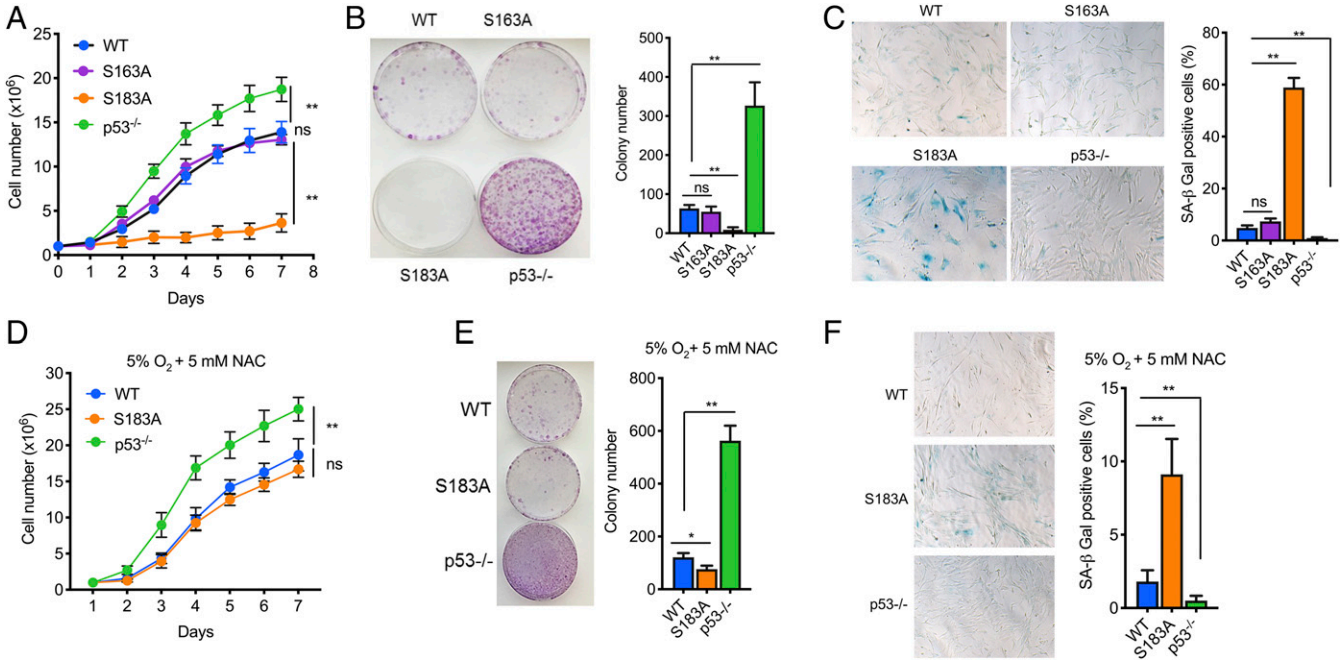

Fig. 1. Loss of Mdm2 Ser183 phosphorylation promotes premature senescence. (*A*–*C*) MEFs were cultured at 21% oxygen. (*A*) Proliferation of passage 3 MEFs ($n = 3$). (*B*) Representative images of colony formation and colony quantitation in passage 2 MEFs ($n = 3$). (*C*) Representative images showing senescence-associated β-galactosidase staining in passage 3 MEFs and quantitation of positively stained cells ($n = 3$). (*D*–*F*) MEFs were cultured at 5% oxygen in media supplemented with 5 mM NAC. (*D*) Proliferation of passage 3 MEFs ($n = 3$). (*E*) Representative images of colony formation and colony quantitation of passage 2 MEFs ($n = 3$). (*F*) Staining for senescence-associated β-galactosidase and quantitation of positively stained MEFs ($n = 3$). Data is expressed as mean ± SD. Student's *t* test $*P < 0.05$, $**P < 0.01$, and ns: not significant.

senescence in Mdm2^{S183A} MEFs at high oxygen is likely due to the increased levels of p53 and the expression of senescence-associated p53-target genes. We noticed that p21 mRNA levels at 5% oxygen were similar in WT and Mdm2^{S183A} MEFs, but the protein levels under the same conditions were different (Fig. 2 *C* and *D*). It is possible that phosphorylation of Mdm2 Ser183 may also affect the stability of p21 protein.

Next, we examined whether premature senescence in Mdm2^{S183A} MEFs is p53 dependent. To this end, WT and Mdm2^{S183A} MEFs grown at 21% oxygen were infected with lentivirus expressing HPV-16 E6 protein which induces proteasome-mediated degradation of p53 (23). Expression of E6 in WT and Mdm2^{S183A} MEFs reduced the levels of p53 protein (Fig. 2*E*) and rescued the proliferation defect of Mdm2^{S183A} MEFs to a level similar to that of WT MEFs expressing GFP control (Fig. 2*F*). In addition, loss of p53 expression in Mdm2^{S183A} MEFs rescued these cells from premature senescence (Fig. 2*G*) and facilitated colony formation when the cells were plated at low density (Fig. 2*H*). We obtained similar results when we abrogated p53 expression using p53 shRNA (*SI Appendix*, Fig. S2 *D*–*F*). These data indicate that Mdm2^{S183A} MEFs cultured at 21% oxygen fail to proliferate due to p53-mediated premature senescence.

To investigate why Mdm2^{S183A} MEFs are sensitive to oxygen levels, we first measured ROS levels in these cells using 2′,7′-dichlorofluorescin diacetate (DCFDA) staining. We found that ROS levels in Mdm2^{S183A} MEFs were similar to those in WT and p53$^{-/-}$ MEFs at both high and low oxygen conditions (*SI Appendix*, Fig. S4*A*). This suggests that the proliferative defect observed in Mdm2^{S183A} MEFs cultured at high oxygen is not due to increased production or accumulation of ROS in these mutant cells. Furthermore, Akt was equally activated in WT and Mdm2^{S183A} MEFs grown at high oxygen (*SI Appendix*, Fig. S4*B*), suggesting that ROS activates Akt. To test whether Mdm2^{S183A} MEFs are sensitive to the levels of oxidative stress present when the cells are cultured at high oxygen, we quantified in these cells the amount of malondialdehyde (MDA), a by-product of lipid peroxidation, and 8-Oxo-2-deoxyguanosine, a marker of oxidative DNA damage. We found Mdm2^{S183A} MEFs had higher levels of MDA (*SI Appendix*, Fig. S4*C*) and 8-Oxo-2-deoxyguanosine (*SI Appendix*, Fig. S4*D*) than WT or p53$^{-/-}$ MEFs at high oxygen condition. This difference disappeared when cells were cultured under low oxygen condition, indicating that Mdm2^{S183A} MEFs are sensitive to high levels of oxidative stress present in cells grown at high oxygen conditions. These data indicate that Akt phosphorylation of Mdm2 Ser183 prevents MEFs from undergoing senescence in response to oxidative stress when grown in conventional culture.

Akt Activation Enhances Mdm2 Nuclear Localization, Stability, and p53 Degradation. Concomitant with the increase in p53 proteins in Mdm2^{S183A} MEFs, we observed a decrease in Mdm2 at the protein level, but not at the mRNA level (Fig. 2). This prompted us to investigate how AKT-mediated phosphorylation of Mdm2 Ser183 affects Mdm2 protein levels. Akt is rapidly activated in MEFs when IGF1 is added to serum-starved cells, as shown by the increased phosphorylation of Akt Ser473 and Thr308 (Fig. 3*A*). In WT MEFs, activation of Akt led to a reduction in p53 protein levels and a concomitant increase in Mdm2 protein levels (Fig. 3*A*). In contrast, activation of Akt in Mdm2^{S183A} MEFs did not alter p53 protein levels but led to a time-dependent decline in Mdm2, suggesting that loss of Mdm2 phosphorylation at Ser183 either altered Mdm2 nuclear localization or destabilizes Mdm2, resulting in reduced degradation of p53. To determine whether activation of Akt alters Mdm2 localization in primary cells, we separated nuclear and cytoplasmic fractions of protein lysates extracted from MEFs cultured at low oxygen and stimulated with IGF1 for 2 h. Mdm2 protein levels in the nucleus were significantly higher in WT MEFs versus Mdm2^{S183A} MEFs, and concomitantly, nuclear p53 protein levels in WT MEFs were significantly lower compared to Mdm2^{S183A} MEFs (Fig. 3*B*). Furthermore, inhibition of Akt activity with

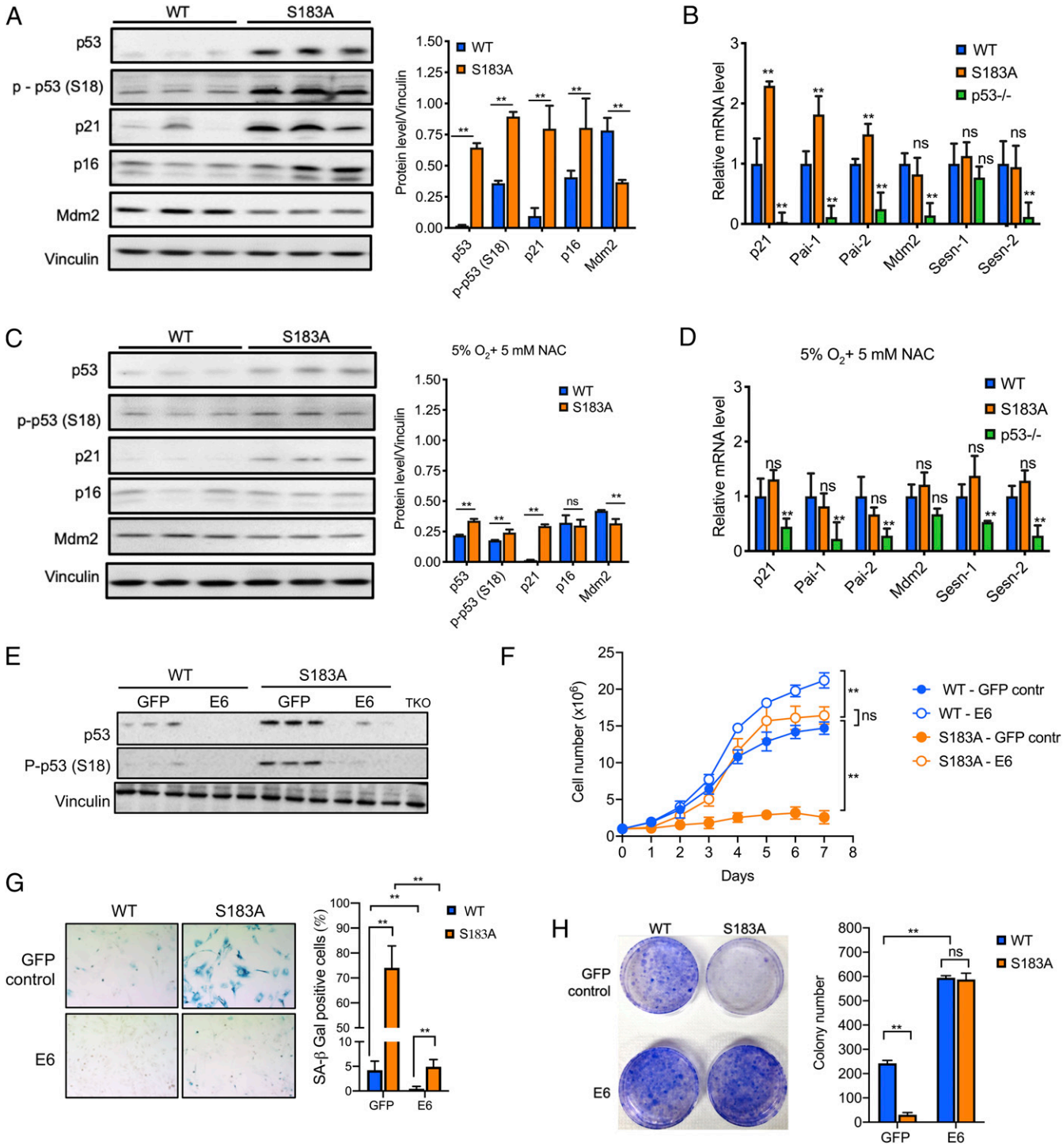

Fig. 2. Premature senescence in Mdm2^{S183A} MEFs is p53 mediated. (*A*) Western analysis of protein lysates from passage 3 MEFs cultured at 21% ($n = 3$). (*B*) RT-qPCR analysis of mRNA expression levels for genes known to mediate senescence in passage 3 MEFs cultured at 21% oxygen ($n = 3$). (*C*) Western analysis of protein lysates from passage 3 MEFs cultured at 5% oxygen in media supplemented with 5 mM NAC ($n = 3$). (*D*) RT-qPCR analysis of MEFs cultured at 5% oxygen in media supplemented with 5 mM NAC ($n = 3$). (*E*) Western analysis for protein lysates extracted from WT and Mdm2^{S183A} MEFs infected with either GFP control or HPV-16 E6 virus at 21% oxygen ($n = 3$). TKO MEFs are deficient for Mdm2, Mdm4, and p53. (*F*) Proliferation assay, (*G*) senescence-associated β-galactosidase staining, and (*H*) colony formation assay for MEFs infected with either GFP control or HPV-16 E6 lentivirus at 21% oxygen ($n = 3$). Data are expressed as mean ± SD. Student's *t* test $^{**}P < 0.01$ and ns: not significant.

MK-2206 resulted in no difference in nuclear Mdm2 and p53 protein levels between WT and Mdm2^{S183A} MEFs (Fig. 3*C*). These data indicate that there is more nuclear Mdm2 when Mdm2 is phosphorylated by Akt, consistent with previous reports (16, 18). However, no concomitant reduction in cytoplasmic Mdm2 protein levels was seen in WT MEFs relative to mutant cells (Fig. 3 *B* and *C*). This finding suggests that Akt phosphorylation of Mdm2-S183 does not impact translocation of

Mdm2 into the nucleus, but rather increases nuclear Mdm2 stability.

We performed cycloheximide pulse-chase experiments to confirm that phosphorylation of Mdm2-Ser183 enhances nuclear Mdm2 stability. After IGF1 stimulation in MEFs cultured at low oxygen with NAC, the half-life of Mdm2 in WT MEFs was 83 min versus 42 min in $Mdm2^{S183A}$ MEFs (Fig. 3*D*), consistent with the observed overall decrease in Mdm2 levels in the mutant cells (Figs. 2 and 3*A*). In WT MEFs, the half-life of cytoplasmic Mdm2 was relatively unchanged (66 min), whereas the half-life of nuclear Mdm2 was 76 min versus 40 min in $Mdm2^{S183A}$ MEFs, revealing that Akt phosphorylation of Mdm2 increases Mdm2 stability in the nucleus. These differences in Mdm2 stability observed in the whole cell and nuclear fractions between WT and $Mdm2^{S183A}$ MEFs were abrogated by inhibiting Akt activation using 5 μM MK-2206 (*SI Appendix*, Fig. S5). These findings suggest that Ser183 phosphorylation in Mdm2 by Akt promotes Mdm2's stability in the nucleus, which subsequently enhances p53 degradation (Fig. 3*B*).

Phosphorylation of Ser183 in Mdm2 Does Not Alter p53-Mediated DNA Damage Response Induced by IR. Our previous studies found that phosphorylation of different residues in Mdm2 exerts differential effects on p53 stabilization and activation in response to ionizing radiation (11, 12, 24). To investigate whether phosphorylation of Ser183 in Mdm2 by Akt alters p53 stabilization and activation in response to DNA damage, we exposed WT and $Mdm2^{S183A}$ MEFs cultured at low oxygen to 4 Gy of ionizing radiation. Overall, there were no significant differences in the levels of p53, activated p53 phosphorylated at Ser18, and p21 proteins between WT and $Mdm2^{S183A}$ MEFs after exposure to IR (Fig. 4*A*). Our findings suggest that phosphorylation of Ser183 in Mdm2 does not affect the level and duration of p53-mediated response after acute DNA damage in vitro.

To further examine the effects of phosphorylation of Ser183 in Mdm2 on p53-mediated cell cycle arrest, we analyzed cell cycle distribution and BrdU incorporation in MEFs cultured at low oxygen following exposure to various DNA damage agents, including ionizing radiation, etoposide, or doxorubicin. Exposure to IR (Fig. 4*B*), doxorubicin, and etoposide (*SI Appendix*, Fig. S6) caused cell cycle arrest in WT and $Mdm2^{S183A}$ MEFs to similar degrees as indicated by the reduced percentage of cells in S phase, while $p53^{-/-}$ control MEFs failed to arrest as expected. Taken together, our data suggest that loss of Akt phosphorylation of Mdm2 does not affect p53 activation and function following acute DNA damage.

Exposure of mice to whole-body ionizing radiation results in p53-mediated apoptosis in bone marrow and other radiosensitive tissues such as the spleen and thymus (25). Therefore, we examined apoptosis in the spleen and thymus of mice exposed to 5 Gy of ionizing radiation. We found that the percentage of apoptotic cells in spleen and thymus of $Mdm2^{S183A}$ mice was comparable to that seen in WT mice (Fig. 4*C*). To determine whether phosphorylation of Ser183 in Mdm2 alters p53-mediated DNA damage responses in vivo, we monitored the survival of WT and $Mdm2^{S183A}$ mice exposed to a sublethal dose of ionizing radiation (7.5 Gy). The survival of $Mdm2^{S183A}$ mice and WT mice was similar (Fig. 4*D*). Collectively, our findings indicate that phosphorylation of Ser183 in Mdm2 by Akt does not affect p53-dependent apoptosis and sensitivity to ionizing radiation in vivo.

Phosphorylation of Ser183 in Mdm2 Promotes Tumorigenesis. Since loss of Ser183 phosphorylation in Mdm2 led to an increase in p53 protein levels and p53-mediated senescence in response to oxidative stress, we reasoned that this Mdm2 phosphorylation may alter p53-mediated tumor suppression. We first monitored cohorts of WT and $Mdm2^{S183A}$ mice for tumorigenesis and survival for 35 mo and found that there was no significant difference in tumor-free survival between WT and $Mdm2^{S183A}$ mice (*SI Appendix*, Fig. S7*A*). This is in sharp contrast with our previous results in $Mdm2^{S394A}$ and $Mdm2^{Y393F}$ mice, which are susceptible to spontaneous tumorigenesis (11, 12). During this 35-mo period, 4 out of 22 (18%) WT mice compared with 4 out of 20 (20%) $Mdm2^{S183A}$ mice developed B cell-derived tumors characterized by positive staining for B220 (*SI Appendix*, Fig. S7*B*). None of WT mice and only 1 out of 20 (5%) $Mdm2^{S183A}$ mice presented with T cell-derived tumors with positive CD3 staining (*SI Appendix*, Fig. S7*B*). Collectively, these data demonstrated that Akt-mediated phosphorylation of Ser183 in Mdm2 does not affect spontaneous tumorigenesis in mice.

Since we observed elevated p53 levels and premature senescence in $Mdm2^{S183A}$ cells in the presence of elevated oxidative stress, it is possible that phosphorylation of Ser183 in Mdm2 affects tumorigenesis in the context of oxidative stress. We therefore examined the effect of this phosphorylation on tumorigenesis in a diethylnitrosamine (DEN)-induced liver tumorigenesis model, in which biotransformation of DEN in infant male mice efficiently produces DNA alkylating metabolites and ROS that damage various macromolecules contributing to hepatocarcinogenesis (26, 27). To determine whether there was a difference in ROS generation between WT and $Mdm2^{S183A}$ livers following DEN injection, we stained liver cryosections with a redox-sensitive fluorescent probe dihydroethidium (DHE). The oxidized form of DHE, 2-hydroxyethidium, intercalates with DNA and displays red fluorescence in the nucleus. The levels of fluorescence went up within 24 h after DEN injection, and gradually decreased over the course of a week. We found no apparent differences in the levels of ROS generated between WT and $Mdm2^{S183A}$ livers post DEN exposure (Fig. 5*A*). Further, we did not find a difference between $Mdm2^{S183A}$ and WT livers post DEN exposure in DNA damage, cell proliferation, or apoptosis using γH2A.X, K_i-67, and cleaved Caspase-3 staining (*SI Appendix*, Fig. S8 *A–C*). However, when we analyzed the expression of genes known to mediate senescence, we found that the expression of p16, p21, p-p53(S18), and Pai-1 was significantly elevated in livers of $Mdm2^{S183A}$ mice versus WT mice, starting at 48 h and up until a week after the administration of DEN (Fig. 5 *B* and *C*). These findings suggest that loss of Ser183 phosphorylation in Mdm2 promotes senescence in vivo, likely triggered by the production of ROS after DEN administration.

To determine whether phosphorylation of Ser183 in Mdm2 has an impact on DEN-induced liver tumorigenesis, 2-wk-old WT and $Mdm2^{S183A}$ male mice were injected intraperitoneally with DEN and killed after 40 wk. Upon dissection, 93% of WT mice displayed outwardly visible tumors on the liver compared with 78% of $Mdm2^{S183A}$ mice (Fig. 5*D*). Liver weights, visible tumor number per liver, and total tumor volume per liver were all higher in WT than in $Mdm2^{S183A}$ mice (Fig. 5*E*). Tumors in both WT and $Mdm2^{S183A}$ mice stained positive for glutamine synthetase, a hallmark of hepatocellular carcinoma (HCC) (Fig. 5*F*). Furthermore, pathologic analysis indicated that significantly more WT mice (70.4%) presented with HCC compared with $Mdm2^{S183A}$ mice (26.1%) ($P = 0.0044$) (Fig. 5 *G* and *H*). These findings suggest that Akt phosphorylation of Ser183 in Mdm2 promote the development and progression of DEN-induced HCC, and loss of this phosphorylation sensitizes cells to oxidative stress-induced senescence, which potentially contributes to the suppression of development and progression of DEN-induced liver tumors.

Since previous work established that oncogenic Ras triggers the generation of ROS and promotes cell senescence (28–30), we explored the effects of Akt-Mdm2 signaling on cell growth and cancer in the presence of oncogenic Kras. WT, $Mdm2^{S183A}$, and $p53^{-/-}$ MEFs were cultured at low oxygen and infected with a recombinant retrovirus expressing oncogenic $Hras^{G12V}$. ROS levels were greatly increased in MEFs transduced with $Hras^{G12V}$ relative to levels in MEFs infected with an empty-vector control,

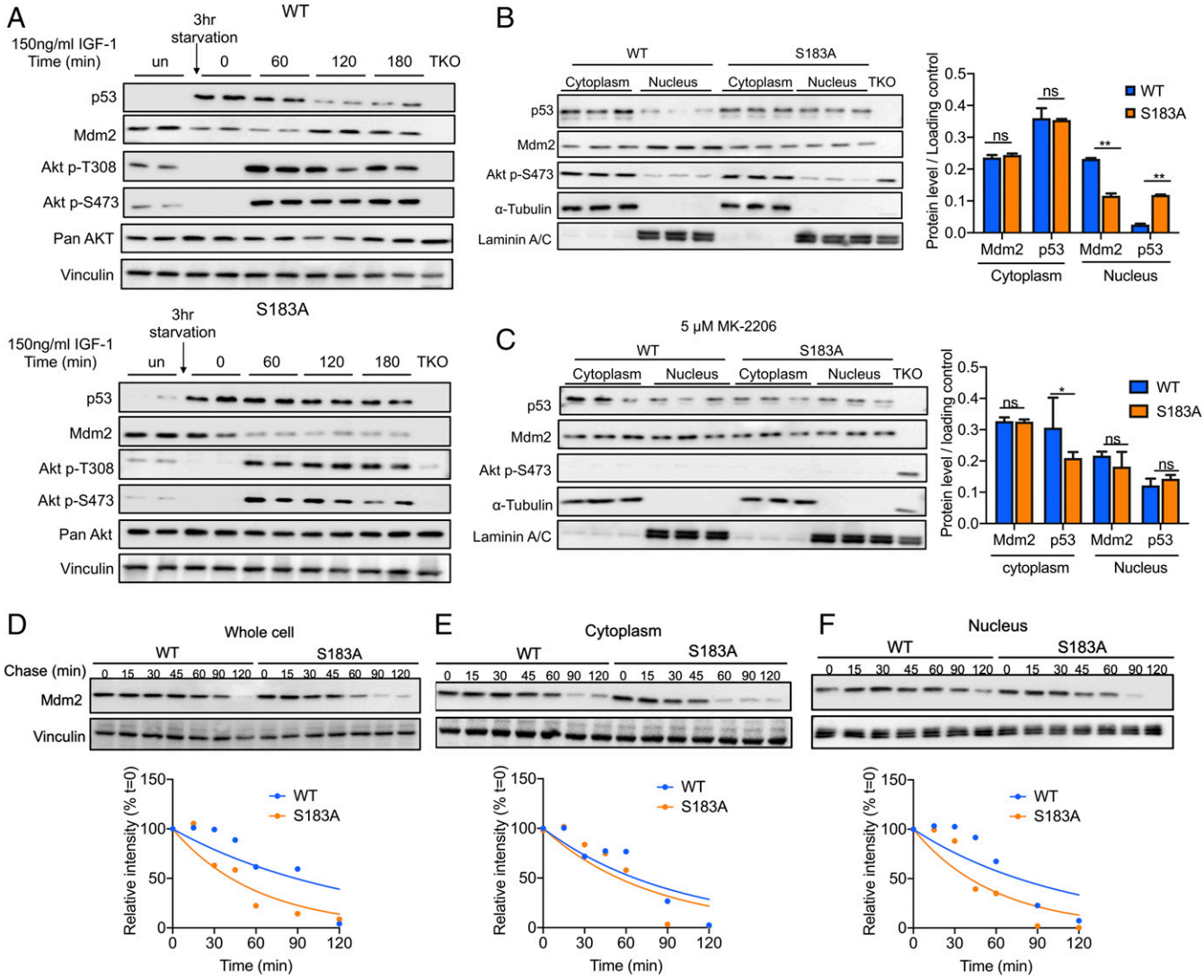

Fig. 3. Phosphorylation of Mdm2 Ser183 by Akt alters Mdm2 localization and stabilization. MEFs were cultured at 5% oxygen in media supplemented with 5 mM NAC. (*A*) Western blot analysis for passage 2 MEFs. Cells were either left untreated (un) or nutrient starved for 3 h and stimulated with 150 ng/mL IGF1 followed by protein extraction at the indicated time points. Triple knockout cells (TKO) are deficient in Mdm2, Mdm4, and p53. (*B*) Western blot analysis and quantitation for nuclear and cytoplasmic proteins in lysates extracted 2 h post IGF1 treatment from passage 2 MEFs ($n = 3$). (*C*) Western blot analysis and quantitation of nuclear and cytoplasmic proteins in lysates extracted 2 h post IGF1 treatment in the presence of an Akt inhibitor MK-2206 (5 μM) from passage 2 MEFs ($n = 3$). Data are expressed as mean ± SD. Student's *t* test $*P < 0.05$, $**P < 0.01$, and ns: not significant. (*D–F*) Western blot analysis and quantitation of proteins in (*D*) whole cell, (*E*) cytoplasmic, and (*F*) nuclear fractions of lysates from MEFs treated with 100 μg/mL cycloheximide and harvested at the indicated time points. Mdm2 levels were normalized to loading control and data were fitted on one curve decay plots.

with the elevation of ROS levels similar among WT, $Mdm2^{S183A}$, and $p53^{-/-}$ MEFs (Fig. 6*A*). In MEFs transduced with $Hras^{G12V}$, the levels of senescence associated protein such as p53, p-p53(S18), and p16 were elevated compared with vector-transfected MEFs (Fig. 6*C*). However, p21 protein levels were higher in $Mdm2^{S183A}$ MEFs expressing $Hras^{G12V}$ than in WT MEFs expressing $Hras^{G12V}$ (Fig. 6*B*), and the percentage of cells positive for SA-β-gal staining was also higher in $Mdm2^{S183A}$ MEFs than in WT MEFs (Fig. 6*B*), consistent with the notion that $Mdm2^{S183A}$ MEFs are more sensitive to oxidative stress-induced senescence.

We next examined the effects of Akt phosphorylation of Mdm2-Ser183 in lung tumorigenesis driven by oncogenic Kras. Cohorts of $Kras^{LSL\text{-}G12D}$;$Mdm2^{WT}$ and $Kras^{LSL\text{-}G12D}$;$Mdm2^{S183A}$ mice were generated, and adenovirus expressing Cre recombinase (Ad5-CMV-Cre) was delivered intranasally to the mice at 12 wk of age to activate the expression of $Kras^{G12D}$. Mice were killed at 7.5 mo after adenovirus delivery. We found that $Kras^{G12D}$;$Mdm2^{S183A}$ mice were less prone to lung tumorigenesis than $Kras^{G12D}$;$Mdm2^{WT}$ mice and had a lower tumor burden (Fig. 6*D*). Moreover, the percentage of mice that presented with carcinomas was significantly higher in $Kras^{G12D}$;$Mdm2^{WT}$ (100%) than those in $Kras^{G12D}$; $Mdm2^{S183A}$ mice (66.6%) ($P = 0.0421$) (Fig. 6*E*). Taken together, our findings indicate that Ser183 phosphorylation in Mdm2 promotes the development and progression of Kras-induced lung tumorigenesis by preventing senescence triggered by elevated ROS characteristic of oncogenic Kras expression.

To further explore the role of Mdm2 Ser183 phosphorylation in a third model of tumorigenesis, we used the two-stage 7,12-dimethylbenz[a]-anthracene (DMBA) and 7,12-dimethylbenz [a]-anthracene (TPA) model to induce the initiation and promotion of epidermal tumors (31). DMBA causes mutations in genes such as Hras in keratinocytes, and TPA promotes the

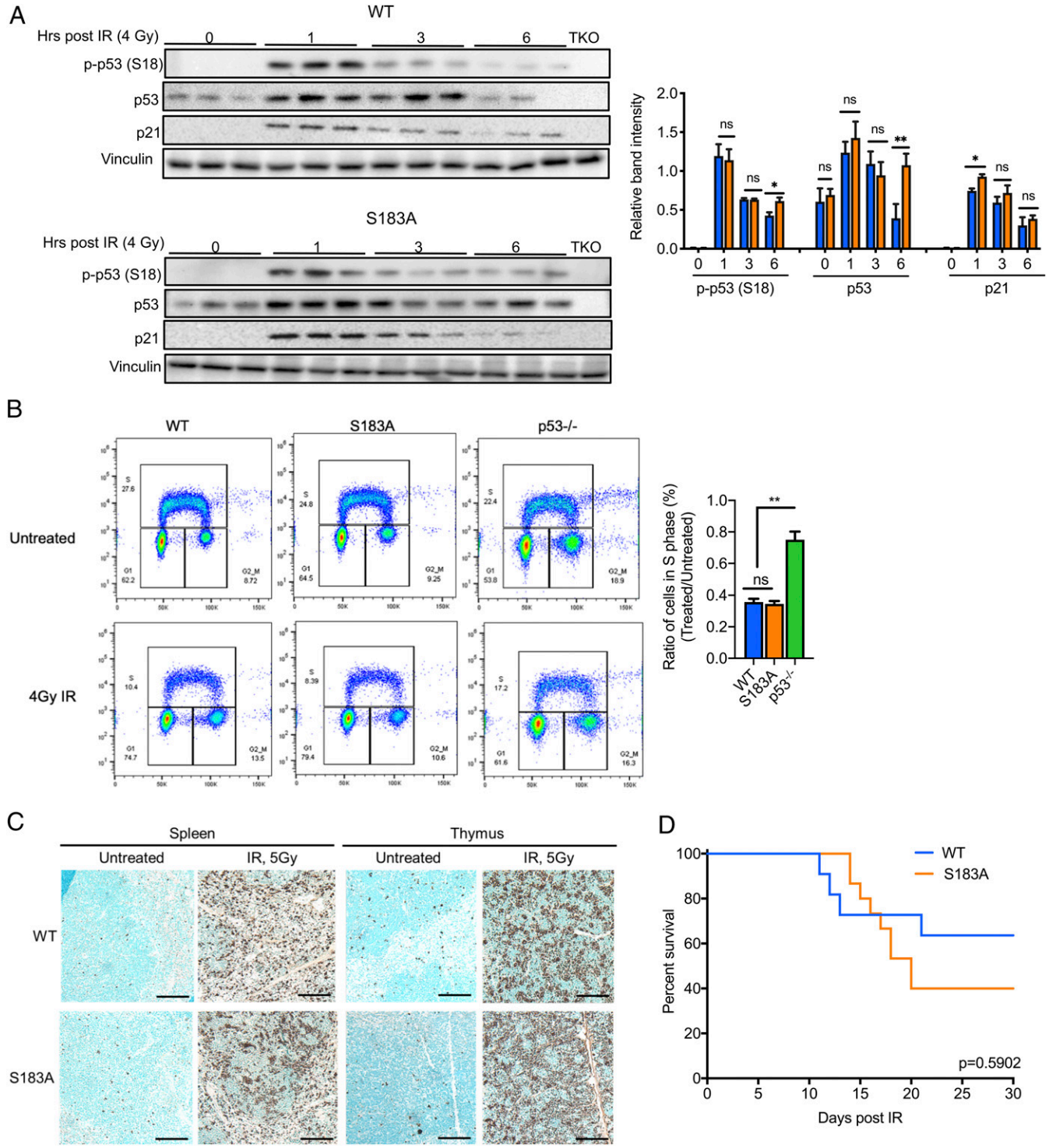

Fig. 4. Mdm2 Ser183 phosphorylation does not affect p53-dependent DNA damage response and survival after IR. MEFs were cultured at 5% oxygen in media supplemented with 5 mM NAC. (*A*) Western analysis of protein lysates collected from passage 2 MEFs treated with 4 Gy IR for the indicated time points. Protein band intensities were quantified for p53, p-p53 (S18), and p21 relative to the loading control protein vinculin. Triple knockout cells (TKO) are deficient in Mdm2, Mdm4, and p53 ($n = 3$). (*B*) Cell cycle analysis presented as the percentage of cells in S phase after exposure to IR and pulse labeling with BrdU and PI ($n = 3$). Data are expressed as mean ± SD. Student's *t* test $^*P < 0.05$, $^{**}P < 0.01$, and ns: not significant. (*C*) TUNEL staining of thymus and spleen harvested from mice 2 h postexposure to IR (5 Gy). (*D*) Survival of WT ($n = 11$) and $Mdm2^{S183A}$ ($n = 15$) mice treated with a sublethal dose of IR (7.5 Gy) and analyzed by log rank test.

clonal expansion of mutant cells and loss of tumor suppressors such as p53, giving rise to skin tumors (31). Additionally, TPA treatment triggers the generation of ROS which causes oxidative damage and inflammation (32, 33). We treated 2-mo-old WT and $Mdm2^{S183A}$ mice by topical application of DMBA followed by biweekly application of TPA for up to 35 wk to promote tumor progression (Fig. 7*A*). Before the appearance of visible papilloma, we stained mouse skin sections for SA-β-gal after

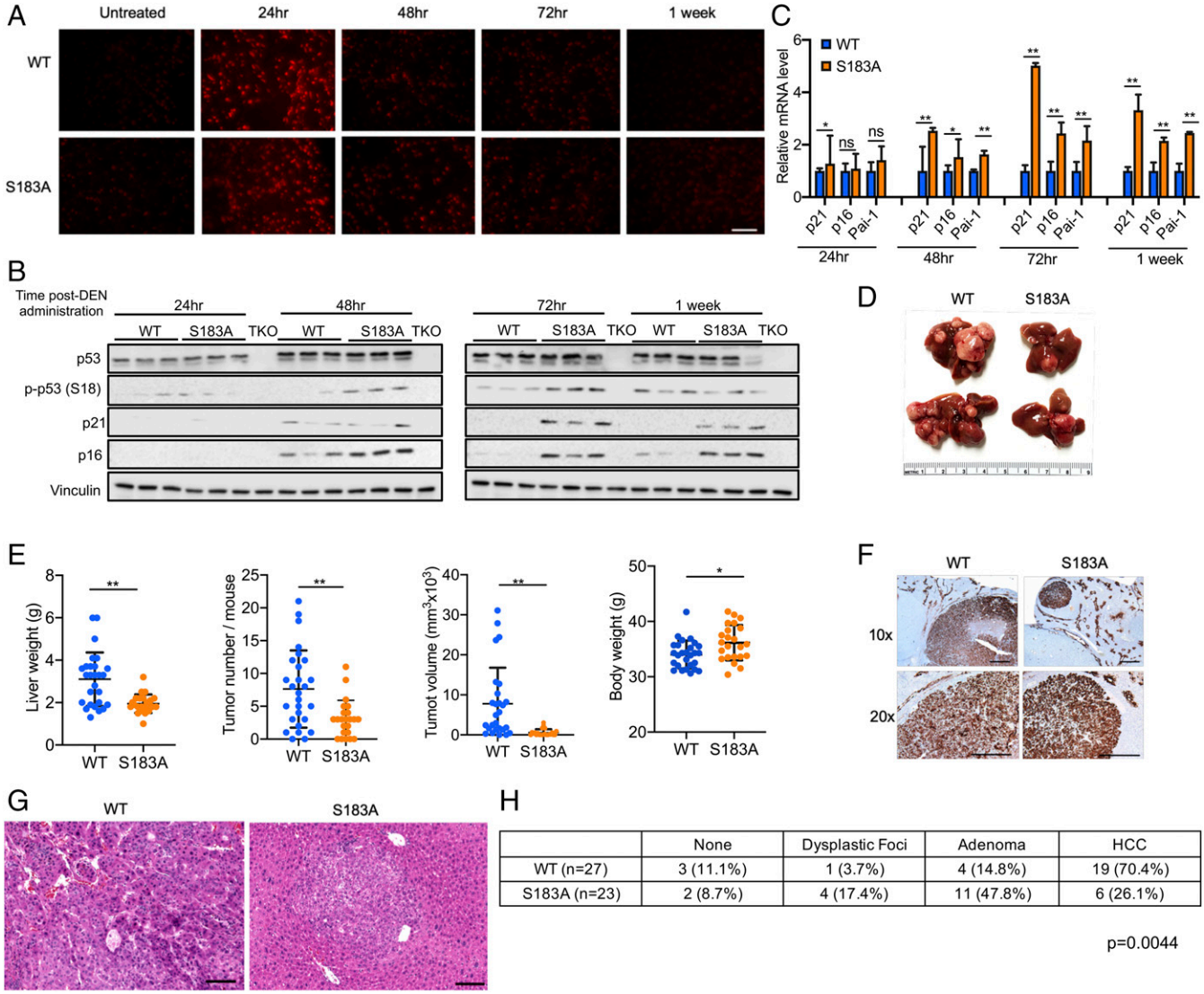

Fig. 5. Phosphorylation of Mdm2 Ser183 promotes DEN-induced liver tumorigenesis. (*A*) Representative images of dihydroethidium staining in liver sections from WT and Mdm2^{S183A} male mice at the indicated time points after DEN administration ($n = 3$). (Scale bar, 20 μm.) (*B*) Western blot analysis of protein lysates from liver tissues harvested from DEN-treated male mice at the indicated time points ($n = 3$). (*C*) RT-qPCR analysis of mRNA expression levels for senescence genes in livers at early time points after DEN treatment ($n = 3$). (*D*) Representative images showing the tumor burden in mice killed 40 wk after DEN was administered at 2 wk of age. (*E*) Body weights, liver weights, tumor numbers, and tumor volumes for both WT ($n = 27$) and Mdm2^{S183A} ($n = 23$) 40 wk after the administration of DEN. (*F*) Representative images showing higher and lower magnification of glutamine synthetase-stained liver sections from 42-wk-old DEN-treated mice. (Scale bar, 100 μm.) Data are expressed as mean ± SD. Student's *t* test $*P < 0.05$, $**P < 0.01$, and ns: not significant. (*G*) Representative H&E staining showing HCC in DEN-treated tumor-bearing mice. (Scale bar, 50 μm.) (*H*) Liver tumors were pathologically classified into dysplastic foci, adenoma, and carcinoma in WT ($n = 27$) and Mdm2^{S183A} ($n = 23$) mice 40 wk after DEN treatment.

DMBA application and at different time points post TPA treatment. We found that senescence was induced in skin 2 wk post TPA treatment in both WT and Mdm2^{S183A} mice, but there was prolonged presence of senescent cells in Mdm2^{S183A} mice compared to WT mice in the first 8 wk of tumor promotion using TPA (Fig. 7*B*).

Next, we performed Western analysis to examine if Mdm2 Ser183 phosphorylation alters senescence markers during the early stages of tumor promotion. We found that p53 protein levels were not significantly different in skin between WT and Mdm2^{S183A} mice in the first 2 wk of TPA application (Fig. 7*C*). However, p53 levels were higher in Mdm2^{S183A} than in WT mice from week 4 to week 8, the time when papillomas first form in WT mice. Phosphorylated p53 (S18), p21, and p16 protein levels were also higher in the skin of Mdm2^{S183A} mice than in WT mice (Fig. 7*C*). These data reveal a more sustained p53-mediated senescence in Mdm2^{S183A} mice compared with WT mice. Senescence is often accompanied by changes in immune cell infiltration, but we did not observe marked differences in the levels of inflammation in WT and Mdm2^{S183A} skin within the first 6 wk of TPA treatment when senescence was detected.

After the emergence of visible papillomas, we measured the number and volume of the tumors. Papillomas first appeared in WT mice 2 mo earlier than in Mdm2^{S183A} mice, and 86.9% of WT mice developed papillomas compared to only 40.9% of Mdm2^{S183A} mice at 35 wk post TPA treatment (Fig. 7 *D* and *E*). The number of papillomas developed in Mdm2^{WT} mice was greater than that in WT mice (Fig. 7*F*). Furthermore, WT mice developed papillomas with larger volumes than Mdm2^{S183A} mice (Fig. 7 *G* and *H*). Collectively, these data indicate that loss of Akt phosphorylation of Mdm2 Ser183 suppresses the initiation and progression of papillomas induced by chemical carcinogens.

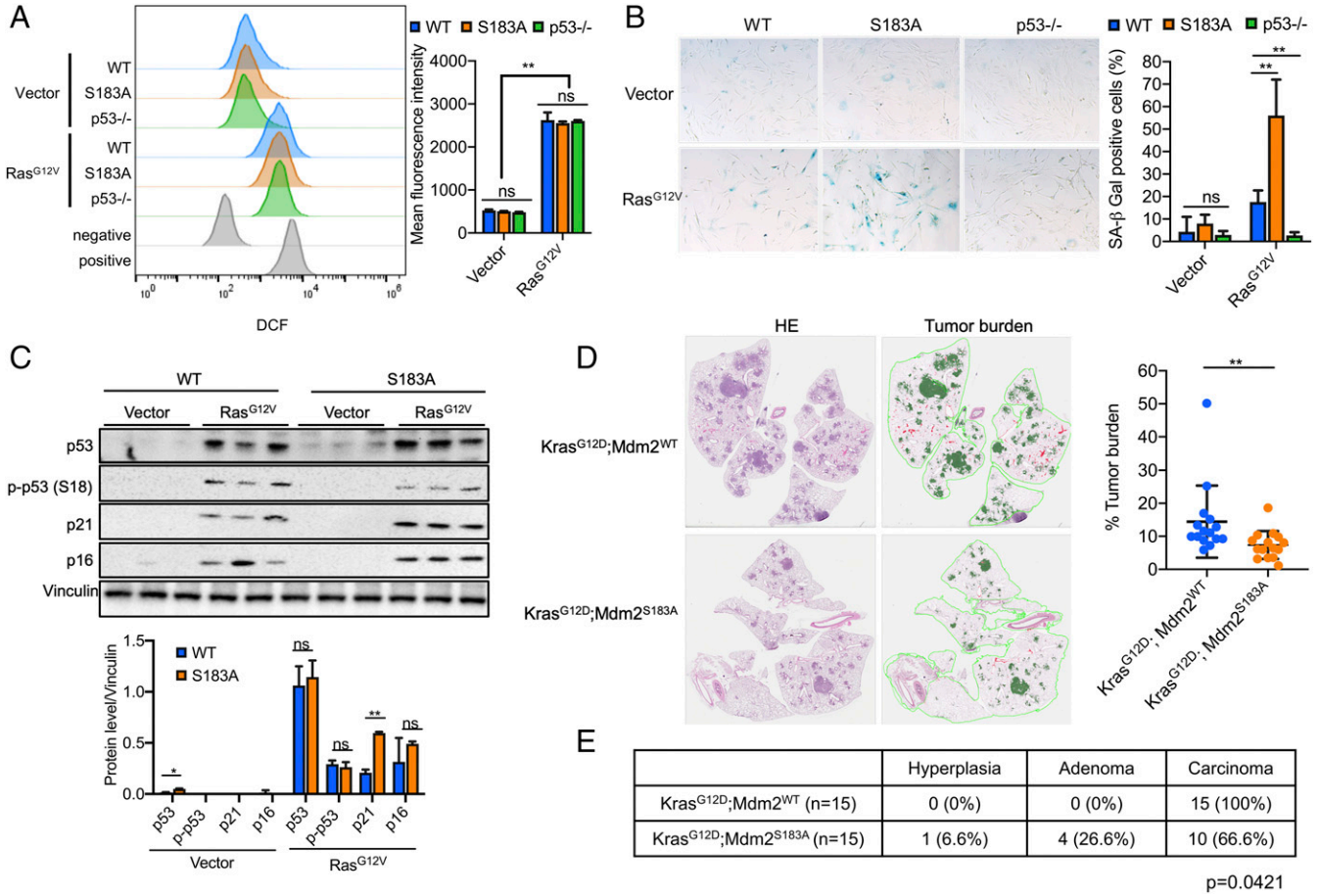

Fig. 6. Mdm2 Ser183 phosphorylation enhances the development of Kras-driven lung tumors. (*A*) Flow cytometry analysis and quantitation of DCF staining in MEFs cultured at 5% oxygen with NAC and transduced with either a pBabe (vector) or its derivative expressing oncogenic $Hras^{G12V}$ ($n = 3$). (*B*) Representative images showing senescence-associated β-galactosidase staining and quantitation of positively stained MEFs cultured at 5% oxygen with NAC and transduced with vector or $Hras^{G12V}$ ($n = 3$). (*C*) Western blot analysis of lysates from MEFs transduced with vector or $Hras^{G12V}$ and band intensities were quantified relative to the loading control protein vinculin ($n = 3$). (*D*) Representative images of H&E-stained lungs from $Kras^{G12D}$;$Mdm2^{WT}$ ($n = 15$) and $Kras^{G12D}$;$Mdm2^{S183A}$ ($n = 15$) at 7.5 mo after Ad-CMV-Cre inhalation. Lung sections were scanned to quantify the area occupied by the tumors. (*E*) Lung tumors were pathologically classified into hyperplasia, adenoma, and carcinoma in lungs harvested 7.5 mo after intubation with Ad-CMV-Cre. Data are expressed as mean ± SD. Student's *t* test $*P < 0.05$, $**P < 0.01$, and ns: not significant.

Discussion

Posttranslational modification of Mdm2 plays a pivotal role in regulating Mdm2-p53 signaling, and phosphorylation of different Mdm2 residues by DNA damage effector kinases has distinct consequences on the p53-mediated DNA damage response, cellular proliferation, and tumorigenesis. We have shown previously that phosphorylation of Ser394 in Mdm2 by ATM destabilizes Mdm2 to increase p53 levels and functions in response to ionizing radiation. Loss of Ser394 phosphorylation in $Mdm2^{S394A}$ mice diminishes p53-mediated apoptosis in cells and tissues following acute DNA damage induced by IR (10). In contrast, phosphorylation of Mdm2 at the adjacent Tyr-393 residue by c-Abl does not alter p53 stability or functions in lymphatic tissues following acute IR (12). However, Mdm2 phosphorylation by both ATM and c-Abl altered IR-induced bone marrow failure and latent tumorigenesis induced by low levels of IR. In this present study, we found that Akt phosphorylation of Mdm2 does not impact p53 activation and function in response to IR, as p53 is similarly stabilized and activated in WT and $Mdm2^{S183A}$ cells after IR damage (Fig. 4*A*), and p53-mediated cell cycle arrest in vitro (Fig. 4*B* and *SI Appendix*, Fig. S6) and apoptosis in vivo (Fig. 4*C*) are unaltered in $Mdm2^{S183A}$ cells and tissues. Instead, we found that loss of Ser183 phosphorylation in Mdm2 sensitizes cells to cellular senescence triggered by chronic exposure to high levels of O_2 (Fig. 1), an effect not observed previously in cells with mutant Mdm2 incapable of being phosphorylated at either or both Ser394 (by ATM) or Tyr393 (by cAbl) (10, 12). These findings highlight the contrasting effects that various effector kinases have on Mdm2 stability, Mdm2-p53 signaling, and the p53-mediated DDR in response to different types of cell stress.

Our findings support a role for Akt signaling to Mdm2 in regulating cell proliferation in response to oxidative stress, which is consistent with the well-established role of Akt in cancer. Akt is often activated in cancer cells, which need to up-regulate antioxidant activities to counteract the increased oxidative stress caused by elevated levels of metabolism (34). The Mdm2 S183A mutation, which prevents Akt phosphorylation at this residue, augments p53-mediated senescence to suppress tumorigenesis. Various physiological and pathological conditions such as aging, ischemia, and cancer lead to increases in oxidative stress (35), which is often countered by intrinsic antioxidant mechanisms to maintain redox homeostasis and ensure cell survival. Since p53 has both pro- and antioxidant properties, the effects of Akt activation on p53 activity through Mdm2 Ser183 phosphorylation may contribute to cell survival. For instance, activation of certain oncogenes such as Kras lead to elevated levels of oxidative stress and kras can cooperate with p53 to induce senescence (36).

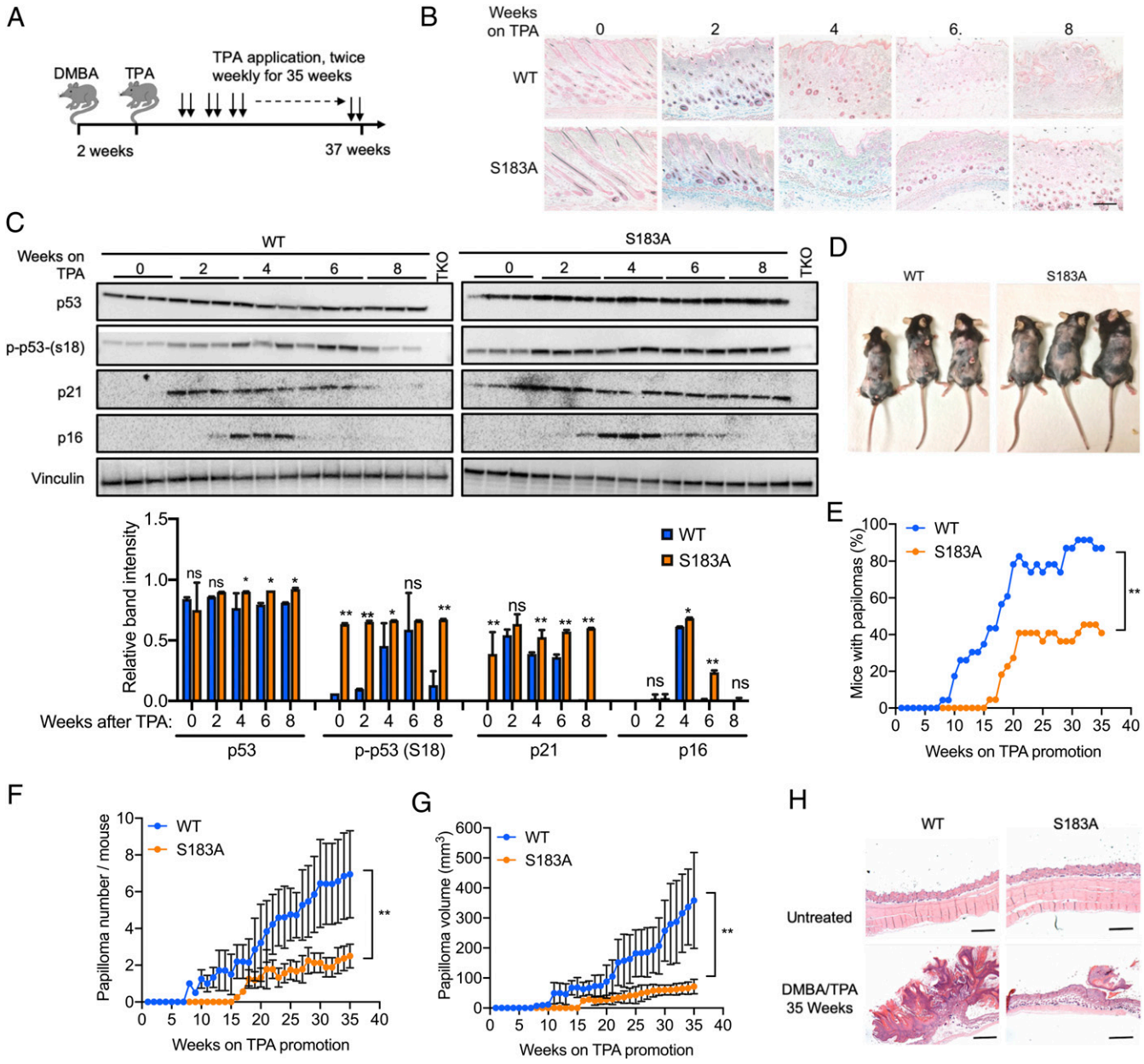

Fig. 7. Mdm2 Ser183 phosphorylation promotes epidermal tumorigenesis. (*A*) Schematic illustration of DMBA/TPA application for skin carcinogenesis protocol. (*B*) Senescence-associated-β-galactosidase staining in skin of mice treated with TPA for the indicated time in weeks. Stained sections were counterstained with Nuclear Fast Red ($n = 3$). (Scale bar, 20 μm.) (*C*) Western analysis and quantitation of proteins from mice skin treated with TPA for the indicated time in weeks ($n = 3$). (*D*) Representative images of mice with papillomas after 32 wk of TPA promotion. (*E*) Percentage of WT ($n = 23$) and $Mdm2^{S183A}$ ($n = 22$) mice with papillomas. (*F*) Number of papillomas per mouse in WT ($n = 23$) and $Mdm2^{S183A}$ ($n = 22$) mice. (*G*) Papilloma volume per mouse in WT ($n = 23$) and $Mdm2^{S183A}$ ($n = 22$) mice. (*H*) Representative H&E staining of papilloma isolated from mice after 32 wk of TPA treatment. (Scale bar, 500 μm.) Data are expressed as mean ± SD. Two-way ANOVA and paired Student's *t* test $*P < 0.05$, $**P < 0.01$, and ns: not significant.

Therefore, the activation of Akt and the subsequent Mdm2 Ser183 phosphorylation in Kras-driven tumors, may promote tumor progression by limiting p53 activity. In future studies, it will be interesting to further dissect which type of ROS are responsible for sensitizing $Mdm2^{S183A}$ MEFs and mice to oxidative stress resulting in p53-mediated senescence as well as examine whether the effects of specific ROS are context dependent.

The effects of $Mdm2^{S183A}$ mutation are in sharp contrast to the $Mdm2^{S394A}$ or $Mdm2^{Y393F}$ mutations, which enhance spontaneous tumorigenesis and tumorigenesis driven by DNA damage or oncogenic signaling in mice (10, 12). Indeed, we found that spontaneous tumorigenesis was unaltered in $Mdm2^{S183A}$ mice (*SI Appendix*, Fig. S7) and, more importantly, that $Mdm2^{S183A}$ mice were less susceptible than WT mice to tumorigenesis driven by oncogenic or carcinogenic signals that trigger ROS generation (Figs. 5–7). In the three tumor models we investigated, ROS plays an important role in tumorigenesis. In the DEN-induced liver tumor model, administration of DEN in infant mice is known to result in elevated levels of oxidative stress (27, 37). We found that liver cells in $Mdm2^{S183A}$ mice are more prone to senescence than WT mice after DEN injection (Fig. 5). Concomitantly, we found that $Mdm2^{S183A}$ mice develop significantly fewer liver tumors and

less aggressive tumors than WT mice, suggesting that the increase in p53-mediated senescence likely contributes to the suppression of DEN-induced liver tumorigenesis in $Mdm2^{S183A}$ mice. This is consistent with findings from a recent study showing that DNA damage triggers Akt phosphorylation of Mdm2 in DEN-induced mouse hepatocellular carcinogenesis (38). In mice, a single injection of DEN leads to acute inflammation, a Kupffer cell response, hepatocyte proliferation, and DNA damage, eventually leading to HCC formation at ~8 to 10 mo of age (39). Hematoxylin and eosin (H&E) examination revealed that both WT and $Mdm2^{S183A}$ mice developed chronic inflammation characterized by presence of mixed population lymphocytes, macrophages, and fibroblasts with lesser numbers of plasma cells and marked circumferential fibrosis. However, differences in immune cell infiltration were minimal between WT and $Mdm2^{S183A}$ tumors (65% in WT and 69% in $Mdm2^{S183A}$).

Oncogenic $Hras^{G12V}$ is known to promote ROS accumulation and cooperate with p53 expression to trigger senescence (36). We found that $Mdm2^{S183A}$ MEFs are more sensitive than WT cells to $Hras^{G12V}$-induced senescence, while $Mdm2^{S183A}$ mice were less prone than WT mice to lung tumorigenesis driven by the oncogenic $Kras^{G12D}$ (Fig. 6). Similarly, topical administration of TPA is known to trigger oxidative stress that causes oxidative damage and inflammation (32, 40). We found increased senescence in the skin of $Mdm2^{S183A}$ mice after DMBA/TPA treatment. Conversely, $Mdm2^{S183A}$ mice were significantly less susceptible to papilloma development, with greatly reduced tumor latency, penetrance, and growth (Fig. 7). Taken together, our studies indicate that loss of Ser183 phosphorylation in Mdm2 enhances p53-mediated senescence in response to oxidative stress, which likely serves a tumor suppression mechanism in carcinogen-induced or oncogene-driven tumorigenesis in liver, lung, and skin.

Phosphorylation of Mdm2 can trigger Mdm2 ubiquitination and destabilization (10, 11, 41). For instance, ATM phosphorylates and promotes nuclear localization of casein kinase I (CKI) (42), which can phosphorylate Mdm2 at multiple serine residues to facilitate Mdm2-SCF (beta-TRCP) interactions, Mdm2 ubiquitination, and subsequent Mdm2 degradation in the 26S proteasome (43). This suggests that phosphorylated Mdm2 is a target for E3 ligases following exposure to cellular stress. We found that $Mdm2^{S183A}$ protein is less stable than WT Mdm2 upon Akt activation (Fig. 3), in keeping with previous studies showing that transfected Mdm2 capable of being phosphorylated by Akt at Ser166/186 (44) or Ser166/188 (45) is more stable. How Akt-mediated phosphorylation of Mdm2 enhances Mdm2 stability is not clearly understood. We found that upon Akt activation, the nuclear fraction of Mdm2 in WT cells is increased compared to that in $Mdm2^{S183A}$ cells (Fig. 3). An increase in nuclear Mdm2 abundance upon Akt activation could be the result of enhanced nuclear translocation of Ser183-phosphorylated Mdm2, as suggested by previous transfection-based studies (16, 18). However, the cytoplasmic fraction of Mdm2 is similar between WT and $Mdm2^{S183A}$ cells (Fig. 3), suggesting that Akt phosphorylation of Mdm2 Ser183 may increase Mdm2 levels by protecting nuclear Mdm2 from ubiquitination and proteasomal degradation. Interestingly, a decrease in nuclear Mdm2 stability in the $Mdm2^{S183A}$ model has a selective impact on p53 activities and triggers p53-mediated senescence without altering p53 apoptosis. This suggests that additional p53 signals induced by other forms of cell stress (such as IR) are required to unleash the full p53-mediated DDR in $Mdm2^{S183A}$ cells and mice.

Developmentally, $Mdm2^{S163A}$ and $Mdm2^{S183A}$ mice are phenotypically indistinguishable from WT mice. Thus, Akt-mediated Mdm2 phosphorylation does not affect embryonic development or organismal growth under normal physiologic conditions (*SI Appendix*, Fig. S1). Furthermore, there are minimal differences in p53 levels and functions in WT and $Mdm2^{S183A}$ MEFs when cultured under normoxic conditions. Surprisingly, multiple attempts to generate both mutations ($Mdm2^{S163A/S183A}$) in cis on the same allele failed, even when attempted by conventional gene targeting strategies using homologous recombination in embryonic stem (ES) cells, suggesting that loss of phosphorylation of both residues may be cell lethal. Although only $Mdm2^{S183A}$ MEFs displayed the profound premature senescence phenotype in culture, it is possible that phosphorylation of the Mdm2-S163 residue also contributes to Akt regulation of the Mdm2-p53 signaling axis in mice, and that blocking both Mdm2 Ser183 and Mdm2 Ser163 phosphorylation by Akt will lead to even more robust p53 activation and tumor suppression in response to DNA damage induced by oxidative stress. Based upon this premise and the results of our study, blocking phosphorylation of one or both of these Akt-target residues on Mdm2 may open a new avenue to activate p53 for cancer treatment.

Materials and Methods

Details of all materials including a list of reagents such as antibodies, mouse strains, primers for RT-qPCR, and oligo sequences for CRSPR-mediated gene editing for our studies can be found in *SI Appendix*. All methods detailing experiments including senescence-associated β-galactosidase staining, colony formation assay, DCFDA assay, cell cycle analysis, lipid peroxidation assay, apoptosis assay, retroviral- and lentiviral-mediated gene transfer, immunofluorescence, immunoblotting, and immunohistochemistry can also be found in the *SI Appendix*.

All animal experimental procedures were reviewed and approved by the Institutional Animal Care and Use Committee of University of Massachusetts Medical School.

Data Availability. All study data are included in the article and supporting information.

ACKNOWLEDGMENTS. This study is supported by NIH Grant R01CA077735 to S.N.J. and H.Z.

1. D. Malkin *et al.*, Germ line p53 mutations in a familial syndrome of breast cancer, sarcomas, and other neoplasms. *Science* **250**, 1233–1238 (1990).
2. K. H. Vousden, X. Lu, Live or let die: The cell's response to p53. *Nat. Rev. Cancer* **2**, 594–604 (2002).
3. R. Stad *et al.*, Hdmx stabilizes Mdm2 and p53. *J. Biol. Chem.* **275**, 28039–28044 (2000).
4. S. D. Boyd, K. Y. Tsai, T. Jacks, An intact HDM2 RING-finger domain is required for nuclear exclusion of p53. *Nat. Cell Biol.* **2**, 563–568 (2000).
5. R. Honda, H. Tanaka, H. Yasuda, Oncoprotein MDM2 is a ubiquitin ligase E3 for tumor suppressor p53. *FEBS Lett.* **420**, 25–27 (1997).
6. X. Wu, J. H. Bayle, D. Olson, A. J. Levine, The p53-mdm-2 autoregulatory feedback loop. *Genes Dev.* **7**, 1126–1132 (1993).
7. H. S. Gannon, S. N. Jones, Using mouse models to explore MDM-p53 signaling in development, cell growth, and tumorigenesis. *Genes Cancer* **3**, 209–218 (2012).
8. H. K. Sluss, H. Armata, J. Gallant, S. N. Jones, Phosphorylation of serine 18 regulates distinct p53 functions in mice. *Mol. Cell. Biol.* **24**, 976–984 (2004).
9. C. Chao, D. Herr, J. Chun, Y. Xu, Ser18 and 23 phosphorylation is required for p53-dependent apoptosis and tumor suppression. *EMBO J.* **25**, 2615–2622 (2006).
10. H. S. Gannon, B. A. Woda, S. N. Jones, ATM phosphorylation of Mdm2 Ser394 regulates the amplitude and duration of the DNA damage response in mice. *Cancer Cell* **21**, 668–679 (2012).
11. M. I. Carr, J. E. Roderick, H. S. Gannon, M. A. Kelliher, S. N. Jones, Mdm2 phosphorylation regulates its stability and has contrasting effects on oncogene and radiation-induced tumorigenesis. *Cell Rep.* **16**, 2618–2629 (2016).
12. M. I. Carr *et al.*, Phosphorylation of the Mdm2 oncoprotein by the c-Abl tyrosine kinase regulates p53 tumor suppression and the radiosensitivity of mice. *Proc. Natl. Acad. Sci. U.S.A.* **113**, 15024–15029 (2016).
13. B. D. Manning, A. Toker, AKT/PKB signaling: Navigating the network. *Cell* **169**, 381–405 (2017).
14. Q. Liu, K. M. Turner, W. K. Alfred Yung, K. Chen, W. Zhang, Role of AKT signaling in DNA repair and clinical response to cancer therapy. *Neuro-oncol.* **16**, 1313–1323 (2014).
15. H. F. Li, J. S. Kim, T. Waldman, Radiation-induced Akt activation modulates radioresistance in human glioblastoma cells. *Radiat. Oncol.* **4**, 43 (2009).
16. L. D. Mayo, D. B. Donner, A phosphatidylinositol 3-kinase/Akt pathway promotes translocation of Mdm2 from the cytoplasm to the nucleus. *Proc. Natl. Acad. Sci. U.S.A.* **98**, 11598–11603 (2001).
17. Y. Ogawara *et al.*, Akt enhances Mdm2-mediated ubiquitination and degradation of p53. *J. Biol. Chem.* **277**, 21843–21850 (2002).

18. B. P. Zhou *et al*., HER-2/neu induces p53 ubiquitination via Akt-mediated MDM2 phosphorylation. *Nat. Cell Biol.* **3**, 973–982 (2001).
19. S. N. Jones, A. E. Roe, L. A. Donehower, A. Bradley, Rescue of embryonic lethality in Mdm2-deficient mice by absence of p53. *Nature* **378**, 206–208 (1995).
20. R. Montes de Oca Luna, D. S. Wagner, G. Lozano, Rescue of early embryonic lethality in mdm2-deficient mice by deletion of p53. *Nature* **378**, 203–206 (1995).
21. V. Nogueira *et al*., Akt determines replicative senescence and oxidative or oncogenic premature senescence and sensitizes cells to oxidative apoptosis. *Cancer Cell* **14**, 458–470 (2008).
22. D. McHugh, J. Gil, Senescence and aging: Causes, consequences, and therapeutic avenues. *J. Cell Biol.* **217**, 65–77 (2018).
23. J. W. Yi, M. Jang, S. J. Kim, S. S. Kim, J. E. Rhee, Degradation of p53 by natural variants of the E6 protein of human papillomavirus type 16. *Oncol. Rep.* **29**, 1617–1622 (2013).
24. H. S. Gannon, L. A. Donehower, S. Lyle, S. N. Jones, Mdm2-p53 signaling regulates epidermal stem cell senescence and premature aging phenotypes in mouse skin. *Dev. Biol.* **353**, 1–9 (2011).
25. E. A. Komarova *et al*., Dual effect of p53 on radiation sensitivity in vivo: p53 promotes hematopoietic injury, but protects from gastro-intestinal syndrome in mice. *Oncogene* **23**, 3265–3271 (2004).
26. L. Verna, J. Whysner, G. M. Williams, N-nitrosodiethylamine mechanistic data and risk assessment: Bioactivation, DNA-adduct formation, mutagenicity, and tumor initiation. *Pharmacol. Ther.* **71**, 57–81 (1996).
27. P. Cerutti, R. Ghosh, Y. Oya, P. Amstad, The role of the cellular antioxidant defense in oxidant carcinogenesis. *Environ. Health Perspect.* **102** (suppl. 10), 123–129 (1994).
28. A. C. Lee *et al*., Ras proteins induce senescence by altering the intracellular levels of reactive oxygen species. *J. Biol. Chem.* **274**, 7936–7940 (1999).
29. R. Colavitti, T. Finkel, Reactive oxygen species as mediators of cellular senescence. *IUBMB Life* **57**, 277–281 (2005).
30. M. Serrano, A. W. Lin, M. E. McCurrach, D. Beach, S. W. Lowe, Oncogenic ras provokes premature cell senescence associated with accumulation of p53 and p16INK4a. *Cell* **88**, 593–602 (1997).
31. E. L. Abel, J. M. Angel, K. Kiguchi, J. DiGiovanni, Multi-stage chemical carcinogenesis in mouse skin: Fundamentals and applications. *Nat. Protoc.* **4**, 1350–1362 (2009).
32. E. M. Perchellet, N. L. Abney, J. P. Perchellet, Stimulation of hydroperoxide generation in mouse skins treated with tumor-promoting or carcinogenic agents in vivo and in vitro. *Cancer Lett.* **42**, 169–177 (1988).
33. J. P. Perchellet, E. M. Perchellet, Antioxidants and multistage carcinogenesis in mouse skin. *Free Radic. Biol. Med.* **7**, 377–408 (1989).
34. N. Koundouros, G. Poulogiannis, Phosphoinositide 3-kinase/Akt signaling and redox metabolism in cancer. *Front. Oncol.* **8**, 160 (2018).
35. G. Pizzino *et al*., Oxidative stress: Harms and benefits for human Health. *Oxid. Med. Cell. Longev.* **2017**, 8416763 (2017).
36. G. Ferbeyre *et al*., Oncogenic ras and p53 cooperate to induce cellular senescence. *Mol. Cell. Biol.* **22**, 3497–3508 (2002).
37. Y. Sánchez-Pérez *et al*., Oxidative stress in carcinogenesis. Correlation between lipid peroxidation and induction of preneoplastic lesions in rat hepatocarcinogenesis. *Cancer Lett.* **217**, 25–32 (2005).
38. D. Dhar *et al*., Liver cancer initiation requires p53 inhibition by CD44-enhanced growth factor signaling. *Cancer Cell* **33**, 1061–1077.e6 (2018).
39. S. I. Grivennikov, F. R. Greten, M. Karin, Immunity, inflammation, and cancer. *Cell* **140**, 883–899 (2010).
40. Y. Nakamura *et al*., A diacetylenic spiroketal enol ether epoxide, AL-1, from Artemisia lactiflora inhibits 12-O-tetradecanoylphorbol-13-acetate-induced tumor promotion possibly by suppression of oxidative stress. *Cancer Lett.* **140**, 37–45 (1999).
41. D. W. Meek, T. R. Hupp, The regulation of MDM2 by multisite phosphorylation–opportunities for molecular-based intervention to target tumours? *Semin. Cancer Biol.* **20**, 19–28 (2010).
42. Z. Wang *et al*., DNA damage-induced activation of ATM promotes β-TRCP-mediated Mdm2 ubiquitination and destruction. *Oncotarget* **3**, 1026–1035 (2012).
43. H. Inuzuka *et al*., Phosphorylation by casein kinase I promotes the turnover of the Mdm2 oncoprotein via the SCF(beta-TRCP) ubiquitin ligase. *Cancer Cell* **18**, 147–159 (2010).
44. M. Ashcroft *et al*., Phosphorylation of HDM2 by Akt. *Oncogene* **21**, 1955–1962 (2002).
45. J. Feng *et al*., Stabilization of Mdm2 via decreased ubiquitination is mediated by protein kinase B/Akt-dependent phosphorylation. *J. Biol. Chem.* **279**, 35510–35517 (2004).
46. H. Zhang, S. N. Cohen, Smurf2 up-regulation activates telomere-dependent senescence. *Genes Dev.* **18**, 3028–3040 (2004).
47. A. Ventura *et al*., Cre-lox-regulated conditional RNA interference from transgenes. *Proc. Natl. Acad. Sci. U.S.A.* **101**, 10380–10385 (2004).
48. E. L. Jackson *et al*., The differential effects of mutant p53 alleles on advanced murine lung cancer. *Cancer Res.* **65**, 10280–10288 (2005).
49. Y. E. Greer *et al*., MEDI3039, a novel highly potent tumor necrosis factor (TNF)-related apoptosis-inducing ligand (TRAIL) receptor 2 agonist, causes regression of orthotopic tumors and inhibits outgrowth of metastatic triple-negative breast cancer. *Breast Cancer Res.* **21**, 27 (2019).